PHYSICAL REVIEW E VOLUME 49, NUMBER 6 JUNE 1994

Interaction of subpicosecond KrF laser pulses with a preformed carbon plasma

W. Theobald, C. Wülker, J. Jasny,* S. Szatmári,† and F. P. Schäfer
Abteilung Laserphysik, Max-Planck-Institut für biophysikalische Chemie, Postfach 28 41,D-37018 Göttingen, Germany

J. S. Bakos
Department of Plasma Physics, Research Institute for Particle and Nuclear Physics, P. O. Box 49, H-1525 Budapest, Hungary

(Received 27 September 1993)

Spectra produced by high-intensity, subpicosecond KrF laser pulses in a preformed carbon plasma are measured in the 10–700 Å spectral range. These spectra differ from those produced on the surface of a solid without a preplasma. The main change in the spectra is explained by the field ionization of atoms and ions of the preplasma as a dominant mechanism of interaction.

PACS number(s): 52.40.Nk, 52.50.Jm, 52.25.Nr

Soft x rays produced by a laser are generated, usually, in a plasma on the surface of a solid material. The intensity and the spectral content of the emitted radiation decisively depend on the details of the laser-plasma interaction processes and on the features of the plasma formed. To increase the efficiency of the x-ray generation in a predetermined spectral region the plasma properties have to be tailored appropriately. For this purpose preformed plasmas generated by prepulses of laser radiation have been used [1,2].

In the case of subpicosecond very high intensity laser radiation interacting with solid material the interaction in fact takes place with a plasma because the high optical field strength transfers the material to the plasma state at the very beginning of the laser pulse. The ions can hardly move during the time of the interaction and therefore the inhomogeneity of the plasma near to the surface of the solid, i.e., the scale length of the plasma, is very short. The scale length of the plasma is defined as $L = n/(dn/dr)$ where n is the plasma density and r is the space coordinate normal to the irradiated surface.

The result of the presence of a prepulse is that the scale length of the plasma will be longer than without it because of the hydrodynamic expansion during the time between the prepulse and the main pulse. The interaction with the plasma, i.e., the absorption of radiation, the rate of the various atomic relaxation processes, and consequently the plasma emissivity will change with the changing scale length [3–5].

In recent experiments an increase of the soft x-ray radiation intensity by a maximum of about a factor of 3 was detected [1,2,5]. This increase is explained by increased collisional absorption near the critical surface [5] or by the increase of the volume of the x-ray radiation source because of the larger scale length of the plasma [1]. The critical surface is defined as the surface where the plasma frequency equals the frequency of the driving laser radiation. In one recent experiment using subpicosecond pulses [6] the amplified spontaneous emission (ASE) radiation of a subpicosecond pulse laser system and in another experiment [5] a small fraction of the main subpicosecond pulse was used as the prepulse.

In both cited subpicosecond pulse plasma interaction experiments the scale length of the plasma could be changed only in a limited range. Further investigation of the role of the scale length is clearly justified. In our investigation an increase of the soft x-ray radiation intensity of about a factor of 20 is observed. The increase is explained by field ionization of the preplasma particles which strongly deviates from earlier explanations. This is due to the fact that in the experiment described here a higher laser intensity was used than before.

In this work the time integrated enhancement of the x-ray radiation in the wavelength interval 10–700 Å is investigated with spectral resolution in a preformed carbon plasma. This plasma target is produced by focusing a KrF excimer laser pulse of about 30 ns duration and intensities ranging from 2×10^8 W/cm^2 to 1×10^{10} W/cm^2 on the surface of a highly polished carbon rod. The x rays are produced by shooting a 0.7 ps high-intensity (7×10^{16} W/cm^2) KrF laser pulse into this plasma target. The delay between the leading edge of the long pulse, i.e., the beginning of the plasma formation, and the high-intensity pulse was varied in the range of 0–200 ns.

The geometry of the experiment in vertical and horizontal view is shown in Fig. 1. The target is a highly polished rod of glassy carbon (Sigradur) with a diameter of 5.70 mm. The angles of incidence of the two laser beams to the target normal are 20° and 45° for the long-pulse and the short-pulse laser beam, respectively. The focal spot diameter of the long-pulse beam is 100 μm while that of the short-pulse beam is 5 μm. The sizes of the focal spots of the beams are measured by a beam profiler and a microscope.

The spectrum of the x rays emitted by the plasma as a result of the interaction with the short-pulse beam

*Permanent address: Institute of Physical Chemistry of the Polish Academy of Sciences, ul. Kasprzaka 44/52, 01-224 Warszawa, Poland.

†Permanent address: JATE University, Research Group on Laser Physics of the Hungarian Academy of Sciences, Dóm ter 9, H-6720 Szeged, Hungary.

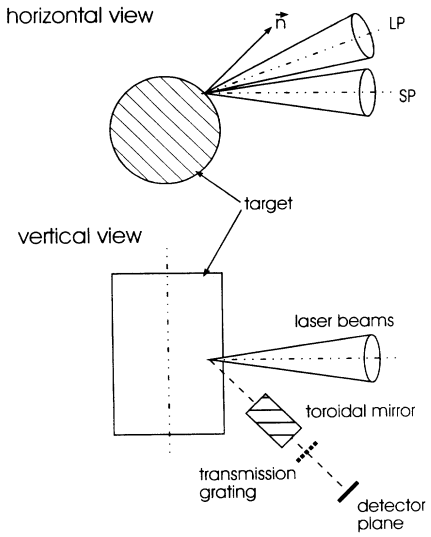

FIG. 1. Sketch of the experimental arrangement. Horizontal view and vertical view. LP: Long pulse beam; SP: short pulse beam.

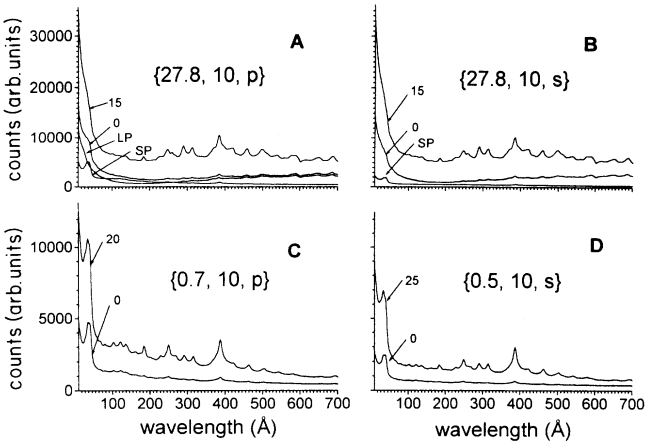

FIG. 2. Soft x-ray spectra. The parameter is the delay of the short pulse in nanoseconds. The spectra labeled LP and SP are the spectra created by the long-pulse and the short-pulse laser alone. The parameter sets given in the figures follow the notation explained in the text.

is measured by a transmission grating spectrograph [7] equipped with a grazing incidence toroidal mirror. The spectrum on the output phosphor screen of a microchannel-plate intensifier is measured by a photodiode array. The observation direction is 45° to the plane containing the target normal and the propagation directions of the two laser beams (Fig. 1).

The short-pulse hybrid dye-KrF excimer laser system is similar to that described in [8] using a three-pass off-axis amplification scheme [9]. The resulting pulse has an energy of up to 20 mJ and 0.5 ps pulse duration. Due to pulse broadening in the windows and lenses, the effective pulse length on the target surface is 0.7 ps. Because of the losses during the propagation of the beam via mirrors to the target chamber the energy of the short pulse (E_{SP}) equals 10 mJ in all of the experiments. The long-pulse beam is produced by a commercial excimer laser (Lambda Physik LPX 100) with a pulse duration of 30 ns. The wavelength of both lasers is 248 nm.

The parameters of the measurement runs are the energy of the long-pulse beam (E_{LP} in mJ), the delay of the short pulse to the leading edge of the long pulse (Δt) in ns, and the polarization direction of the short pulse to the plane of incidence [parallel (p) or perpendicular (s)]. The polarization of the long pulse was always the same and it is not indicated because it plays no role in the physics to be discussed. The timing jitter between the two laser pulses is less than 5 ns. The spectra are measured at various delay times for a given parameter set. The following notation will be used for the parameter sets: $\{E_{LP}, E_{SP}, s/p\}$.

The sensitivity of the spectrograph is high enough to measure a spectrum in a single laser shot. For one parameter set ten spectra are measured and averaged in order to reduce the influence of fluctuations.

Some spectra are shown in Fig. 2. No filter foils are used in front of the spectrograph. The zeroth order diffraction of the transmission grating is not blocked in order not to distort the spectrum artificially at the shorter wavelengths. Thus the increase of intensity below 10 Å is due to the superposition of the zeroth order. A 1000 lines/mm transmission grating is used with a dispersion of 1.5 Å/pixel of the charge-coupled device (CCD) camera.

The parameter indicated in the figures is the delay time between the long and the short pulse in nanoseconds. The short pulse always comes later than the long one. The spectrum enhancement depends on the delay time and has a maximum (see later in Fig. 3). The spectra plotted in Fig. 2 are for no enhancement (zero delay) and maximum enhancement.

The spectrum produced by either the long or the short pulse alone is marked by LP and SP, respectively, in the figure. No LP spectrum can be measured at the 0.7 mJ and 0.5 mJ LP energies [Figs. 2(c) and 2(d)]. The SP spectrum in Fig. 2(c) is the same as in Fig. 2(a) and that of Fig. 2(d) the same as in Fig. 2(b), therefore it is not plotted.

There is a difference in the short-pulse spectra depending on the polarization state [Figs. 2(a), 2(b), curve SP]. The p polarization spectrum is of larger amplitude than the s polarization spectrum in agreement with earlier observations [10]. At low LP energy, the intensity of the enhanced spectrum is also larger for p polarization than for s polarization [Fig. 2(c), curve 20 and Fig. 2(d), curve 25] in contrast to the case of large long pulse energies [Figs. 2(a) and 2(b), curve 15].

Because there is no enhancement at zero delay and no LP spectrum can be detected at small LP energies, the SP spectrum (not shown in the figure) coincides with the zero delay spectrum in Figs. 2(c) and 2(d). However, at 27.8 mJ LP energy, we measure a spectrum produced by the long pulse alone. Therefore the zero delay spectrum is the sum of the long- and short-pulse spectra [Figs. 2(a) and 2(b)].

The change of the spectral content of the enhanced spectra in comparison to the zero delay spectra is very remarkable, especially at longer wavelengths ($\lambda > 100$ Å).

In the case of high long pulse energy the spectral lines with $\lambda < 100$ Å appear only as shoulders on the zeroth order. In the spectral region $\lambda > 100$ Å the enhancement is greater, showing an ensemble of lines. At a first glance the overall shape of the spectrum in this spectral region seems to be not too strongly dependent on the parameters of the experiment.

In order to characterize the complicated change in the spectrum caused by the existence of a preformed plasma, the enhancement spectrum defined as the ratio of the measured spectrum at a defined delay time to the measured spectrum at zero time delay is calculated. The division is made pixel by pixel.

Such an enhancement spectrum can be seen in Fig. 3(a) at the parameter set $\{0.7, 10, p\}$ and at various delays as indicated in nanoseconds. There is an enhancement in the whole spectral region and even an appearance of spectral features showing the detailed structure of the interaction. For example, the C VI and C V lines seem to be relatively depleted, i.e., "absorbed" in the $\lambda < 100$ Å wavelength region while all the other lines are enhanced more than the "continuum." This depletion, i.e., "absorption" cannot be interpreted as real absorption without any assumption about the physical process because this shows only that these lines are not as much enhanced as the "continuum." The cause of this can be a real absorption, i.e., the plasma becomes optically thick for these lines.

The spectrum seems to consist of two parts fusing between 100 to 150 Å . The enhancement maximum in dependence of the delay time already mentioned in connection with Fig. 2 can also be seen in this figure. There is little change in the shape of the spectrum as a function of the delay. The radiation intensity of wavelengths smaller than that of the C VI, C V "absorption lines" is also enhanced, indicating a shift of the maximum of the radiation intensity distribution into the direction of shorter wavelengths in the spectral region $\lambda < 100$ Å .

A similar radiation enhancement spectrum can be seen in Fig. 3(b) at higher prepulse energy, i.e., the parameter set is $\{27.8, 10, s\}$. For maximum enhancement the delay time of the short pulse is 15 ns. At this prepulse energy

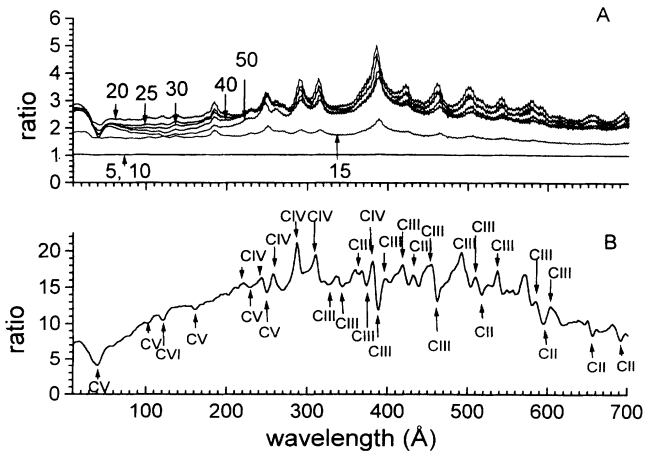

FIG. 3. Radiation enhancement in the preplasma. The ratio is defined in the text. (a) The parameter is the delay of the short pulse. The parameter set is $\{0.7, 10, p\}$. (b) The delay is 15 ns. The parameter set is $\{27.8, 10, s\}$.

there exists a spectrum produced by the long pulse alone. Therefore the division of the spectra by the zero delay spectrum is performed only after the subtraction of the long-pulse spectrum from all the spectra.

The appearance of numerous absorption features indicated by arrows upward together with the ionic state identification is the most remarkable fact besides the overall increase of intensity by a factor of about 20. These show that not only the C VI and C V lines but also the C III and C II lines are absorbed if we assume that the cause of the reduced enhancement, i.e., depletion of these lines is a real absorption in the plasma. It has to be emphasized that all the identified C VI and C V lines are depleted. At the same time all the C IV lines are enhanced. The enhanced lines are marked by arrows downward and the ionic state identification. The C III lines are partly enhanced and partly depleted while the observed C II lines are all depleted. The energies of the lower levels relative to the ionic ground state (C II and C III) of all transitions for which depletion was observed are smaller than 1.3×10^5 cm^{-1} while that of the enhanced C III lines are larger than this value.

Taking into account all the experimental observations given above, a possible description of the interaction of the short pulse with the preformed plasma can be formulated as follows. The short pulse propagates uphill the density gradient of the preformed plasma to the critical density surface and somewhat beyond [4] in the case of a short $L^* = L/\lambda_p < 1$ normalized scale length plasma, where the absorption of the radiation takes place because of resonance absorption and inverse bremsstrahlung. λ_p is the wavelength of the lasers. The position of the heat deposition depends on the scale length of the plasma. At larger scale length it is shifted into the undercritical region. The density of the maximum power deposition is at $n^* = n/n_c \approx 0.3$ at $L^* = 100$ [11].

In the way of the propagation in the undercritical region of the preformed plasma all the atoms and ions are field ionized by the high-intensity short pulse (7×10^{16} W/cm^{-2}) to He like ions in agreement with an estimation using the Ammosov *et al.* expression given by Penetrante and Bardsley [12]. According to this estimation the field ionization rates of C I atoms and C II, C III, and C IV ions are larger than 10^{14} s^{-1}. The recombination of these ions results in the part of the spectrum with wavelengths greater than about 150 Å (long wavelength radiation).

The C^{6+} and C^{5+} ions can be efficiently produced only through collisions in the high density region which is in the case of $L^* = 100$ in the density region of $n/n_c = 0.3$. So an absorption of the short wavelength line radiation is also expected because the plasma can get highly opaque for this radiation. To show this a rough estimate of the opacity of the He_α-line radiation in a plasma of 10^{21} cm^{-3} is now done.

It is assumed that the plasma is dominated by collisions and the excited levels are populated by the Boltzmann distribution. For a homogeneous plasma the emitted intensity is given by $I_\nu(x_0) = [\varepsilon_\nu/\kappa(\nu)](1 - e^{-\kappa(\nu)x_0})$ [13], where ε_ν is the emission coefficient, $\kappa(\nu)$ is the absorption coefficient, and x_0 the plasma thickness. The exponential should be $\kappa(\nu)x_0 \approx 1$ to estimate the thick-

ness. This gives

$$x_0 \approx 8\pi c \frac{\Delta\lambda_{12}}{A_{21} N_1 \lambda_0^4 (1 - e^{-h\nu/kT_e})} ,$$

where N_1 is the ground state population ($\sim 10^{21}$ cm^{-3}), $\lambda_0 = 40.3$ Å (He_α transition), the Einstein coefficient for spontaneous decay is $A_{21} = 8870 \times 10^8$ s^{-1} [14], and $\Delta\lambda_{12} \approx 2 \times 10^{-2}$ Å is the half width assuming a Stark broadened profile [13]. For kT_e we assume a temperature of 300 eV. For x_0 one gets a value of about 0.1 μm. It means that a strong absorption is expected taking into account that the scale length is much larger. The scale length L of the preplasma can be estimated by the formula $L = c_s \Delta t$, where c_s is the ion sound velocity and Δt is the delay of the two laser pulses. The sound velocity c_s depends on the intensity of LP. For a LP energy of 27.8 mJ (10^{10} W/cm^2) one gets according to Ref. [15] a thermal electron temperature of 14.8 eV and a sound velocity of $c_s = 1.5 \times 10^6$ cm/s. L is 150 μm for a delay of $\Delta t = 10$ ns. The scale length is a factor of more than 1500 larger than the estimated absorption length. So the observed depletion in the short wavelength region can be a real absorption.

Increasing the prepulse energy and, consequently, the temperature of the preplasma, the growth of population of lower ionization states in the preplasma is expected with the accompanying absorption of the recombination radiation of the "daughter" ions of C^{4+} ions formed by field ionization. In the geometry of our experiment the plasma produced by the subpicosecond pulse is observed through the surrounding preplasma. Therefore at higher prepulse energies absorption of the line radiation of the carbon atoms of lower ionization state, e.g., C III and C II, is also expected in the preplasma when the corresponding transition ends in a final state of energy smaller than the temperature of the preplasma, since these states are thermally populated. The other lines of transitions ending in a level of higher energy than the thermal limit are enhanced (recombination of C^{3+} and consecutively C^{2+} ions). The estimated temperature of the preplasma formed by the high energy long pulse is about 15 eV according to the 1.3×10^5 cm^{-1} energy of the lower levels of the observed depleted lines in good agreement with the calculated temperature of 14.8 eV.

The increase of the short wavelength radiation can be explained by the increased collisional absorption of the short laser pulse according to earlier experimental observations [5], the decreased collisional relaxation rate and the decreased heat conductivity caused by the longer scale length [3]. The observed intensities of the lines are not increased as much as the continuum because of the absorption.

Some part of the long wavelength radiation originates as the result of collisional and resonance absorption heating around the critical surface due to the longer scale length. The intensity of that part of radiation depends on the energy deposited around the critical surface and, consequently, on the polarization state of the short pulse according to the earlier observations [10]. At larger prepulse energy this part of radiation has a lower intensity than the growing part of intensity emitted by the field ionized particles. Therefore the intensity of the long wavelength radiation becomes independent of the polarization state of the short pulse.

Summarizing our results, field ionization can be stated as one of the dominant interaction mechanisms of a short pulse with a preformed plasma causing an increase of the intensity of soft x-ray radiation by a factor of about 20 in the wavelength interval 150–700 Å .

[1] R. Weber and J. E. Balmer, J. Appl. Phys. **65**, 1880 (1989).

[2] K. A. Tanaka, A. Yamauchi, R. Kodama, T. Mochizuki, T. Yamanaka, S. Nakai, and C. Yamanaka, J. Appl. Phys. **63**, 1787 (1988).

[3] M. M. Murnane, H. C. Kapteyn, and R. W. Falcone, Phys. Rev. Lett. **62**, 155 (1989).

[4] R. Fedosejevs, R. Ottmann, R. Sigel, G. Kühnle, S. Szatmári, and F. P. Schäfer, Phys. Rev. Lett. **64**, 1250 (1990).

[5] U. Teubner, G. Kühnle, and F. P. Schäfer, Appl. Phys. Lett. **59**, 2672 (1991).

[6] C. H. Nam, W. Tighe, E. Valco, and S. Suckewer, Appl. Phys. B **50**, 275 (1990).

[7] J. Jasny, U. Teubner, W. Theobald, C. Wülker, J. Bergmann, and F. P. Schäfer, Rev. Sci. Instrum. (to be published).

[8] S. Szatmári and F. P. Schäfer, Opt. Commun. **68**, 196 (1988).

[9] S. Szatmári, G. Almási, and P. Simon, Appl. Phys. B **53**, 82 (1991).

[10] U. Teubner, J. Bergmann, B. van Wonterghem, F. P. Schäfer, and R. Sauerbrey, Phys. Rev. Lett. **70**, 794 (1993).

[11] For the calculation of the power deposition the computer code of [4] was used.

[12] B. M. Penetrante and J. N. Bardsley, Phys. Rev. A **43**, 3100 (1991); M. V. Ammosov *et al.*, Zh. Eksp. Teor. Fiz. **91**, 2008 (1986) [Sov. Phys. JETP. **64**, 1191 (1986)].

[13] C. DeMichelis and M. Mattioli, Nucl. Fusion **21**, 677 (1981).

[14] W. L. Wiese *et al.*, *Atomic Transition Probabilities, Volume 1, Hydrogen through Neon,* Natl. Bur. Stand. Ref. Data Ser., Natl. Bur. Stand. (U.S.) Circ. No. 4 (U.S. GPO, Washington, DC, 1966).

[15] P. Mora, Phys. Fluids **25**, 6 (1982).